Model for the $\Delta(1600)$ resonance and $\gamma N \to \Delta(1600)$ transition

G. Ramalho[1] and K. Tsushima[2]

[1]*Centro de Física Teórica de Partículas, Av. Rovisco Pais, 1049-001 Lisboa, Portugal*
[2]*Excited Baryon Analysis Center (EBAC) in Theory Center, Thomas Jefferson National Accelerator Facility, Newport News, Virginia 23606, USA*

A covariant spectator constituent quark model is applied to study the $\gamma N \to \Delta(1600)$ transition. Two processes are important in the transition: a photon couples to the individual quarks of the $\Delta(1600)$ core (quark core), and a photon couples to the intermediate pion-baryon states (pion cloud). While the quark core contributions are estimated assuming $\Delta(1600)$ as the first radial excitation of $\Delta(1232)$, the pion cloud contributions are estimated based on an analogy with the $\gamma N \to \Delta(1232)$ transition. To estimate the pion cloud contributions in the $\gamma N \to \Delta(1600)$ transition, we include the relevant intermediate states, πN, $\pi \Delta$, $\pi N(1440)$ and $\pi \Delta(1600)$. Dependence on the four-momentum transfer squared, Q^2, is predicted for the magnetic dipole transition form factor, $G_M^*(Q^2)$, as well as the helicity amplitudes, $A_{1/2}(Q^2)$ and $A_{3/2}(Q^2)$. The results at $Q^2 = 0$ are compared with the existing data.

I. INTRODUCTION

With the extended energy range and the increased precision of recent accelerators, it is now possible to probe the electromagnetic structure of baryon resonances beyond the first resonance region. For example, the facilities like CLAS (Jefferson Lab), MAMI (Mainz), ELSA (Boon), LEGS (Brookhaven), BATES (MIT) and Spring-8 (Japan) are able to measure the electromagnetic transition properties associated with the resonances such as $P_{33}(1232)$, $P_{11}(1440)$, $S_{11}(1535)$ and $D_{13}(1520)$ [1].

To accommodate the data with higher four-momentum transfer squared Q^2 and center-of-mass energy W, an improvement of the data analysis is mandatory, since more baryons and mesons emerge in the possible intermediate states. Then, the exact identification of the resonances easily becomes controversial due to a large number of channels taking place in a very small energy range. Furthermore, the analysis made by various groups, MAID [2], SAID [3], JLab-Yeveran [4,5] JLMS (JLab-Moscow) [6], Bonn-Gatchina [7], Valencia [8], Giessen [9], CMB [10] and KSU [11], is based on different resonance poles and meson-baryon coupling constants. A similar situation exists also for the dynamical coupled-channel reaction models, e.g., Mainz-Taipei [12], Jülich [13,14], and EBAC [15–18] models. One of the most known issues which drives them to study the baryon resonances is the "missing resonance problem," that is, several states predicted by quark models have not yet been observed nor identified by experiments [1,19].

Under such circumstances any theoretical studies for the baryon resonances would help to uncover their properties. For example, $\Delta(1600)$, the first excited state of Δ, may be one of such interesting resonances worthwhile to study. It has not yet been studied well so far. According to the Particle Data Group (PDG) [20] $\Delta(1600)$ is a three-star resonance which decays preferentially to πN, $\pi N(1440)$ and $\pi \Delta$. Although the form factors associated with the electroproduction of this resonance were studied some time ago by a constituent quark model [21], it is only recently that this resonance has been included in meson-baryon reaction analysis models [1,5,7,22]. Recent experiments show that the $\Delta(1600)$ resonance can be very important in double pion production in nucleon-nucleon collisions [23–25]. The $\Delta(1600)$ resonance was also studied in lattice QCD simulations [26,27] and QCD sum rules [28].

Although the experimental access for the $\Delta(1600)$ resonance is still insufficient, it is very interesting to study it theoretically for the following reasons. Similarly to its ground state $\Delta(1232)$, $\Delta(1600)$ can be described as a quark core dressed by a meson cloud in the low Q^2 region. However, contrary to the $\Delta(1232)$ case, meson cloud structure for the $\Delta(1600)$ is expected to be much richer, since more meson-baryon channels are associated with it [20]. To estimate the meson-baryon dressing for the $\Delta(1600)$, one can in principle use dynamical coupled-channel models, but it is also necessary to understand the three-quark core structure based on the underlying physics of QCD, instead of using a phenomenological parametrization. Thus, the use of a quark model, which includes the degrees of freedom that dominate in the intermediate and higher Q^2 region generally, is a natural consequence. Quark models have also proven to be very useful in the studies of nucleon and $\Delta(1232)$ systems.

In this article we study the structure of $\Delta(1600)$ and the $\gamma N \to \Delta(1600)$ transition, by applying a covariant spectator constituent quark model [29–39]. In this model one can naturally assume the $\Delta(1600)$ as the first radial excitation of $\Delta(1232)$, similarly to the case of $N(1440)$ and N [34]. The interpretation of the $\Delta(1600)$ resonance as the first radial excitation of $\Delta(1232)$ is sufficient for the present approach to estimate the valence quark contributions for

the $\gamma N \rightarrow \Delta(1600)$ transition. No extra parameters are required. However, the transitions $\gamma N \rightarrow \Delta(1232)$ and $\gamma N \rightarrow \Delta(1600)$, are very different with respect to the pion cloud effects. While the pion cloud contributions are about 30–45% for the transition with the $\Delta(1232)$, the pion cloud contributions would be more significant for the transition with the $\Delta(1600)$. This is due to the increase of relevant intermediate states, πN, $\pi \Delta$, $\pi N(1440)$ and $\pi \Delta(1600)$.

Before discussing any details of the numerical results, we can state that, solely from the quark core contributions, the magnetic dipole transition form factors in the $\gamma N \rightarrow \Delta(1600)$ transition at $Q^2 = 0$ are negative (-1.11), and significantly undershoot the experimental data ($\approx +0.20$). However, with the inclusion of the pion cloud contributions which are dominant in the low Q^2 region, the final result approaches to the experimental data points.

This article is organized as follows. In Sec. II general remarks are given for the $\gamma N \rightarrow \Delta$ transitions, and the theoretical background is introduced. In Secs. III and IV contributions from the valence quarks and pion cloud are, respectively, discussed for the $\gamma N \rightarrow \Delta(1600)$ transition. In Sec. V reaction observables are discussed, and their results are presented in Sec. VI. The conclusion is given in Sec. VII.

II. GENERAL REMARKS ON THE $\gamma N \rightarrow \Delta$ TRANSITION

The electromagnetic transition between a spin $1/2$ baryon (e.g., nucleon) and a spin $3/2$ baryon (e.g., Δ) with the positive parity, can be described in terms of three independent form factors introduced by Jones and Scadron [40]: G_M^* (magnetic dipole), G_E^* (electric quadrupole), and G_C^* (Coulomb quadrupole). An example is the $\gamma N \rightarrow \Delta(1232)$ transition.

It is well established that the $\gamma N \rightarrow \Delta(1232)$ transition is dominated by the magnetic dipole form factor, G_M^* [1,31,32,41–44]. This can be easily understood in a naive SU(6) quark model, since $\Delta(1232)$ can be regarded as a system in which one quark spin is flipped from the nucleon system, therefore possible by a pure magnetic dipole transition. In fact, the magnetic dipole form factor, G_M^*, emerges naturally as a dominant form factor when only the S-state structure in the quark-diquark system is included for the $\Delta(1232)$ wave function, and all the remaining form factors vanish [31,41,42]. Although D-states can contribute to the transition, they induce only small corrections for G_M^*, besides the contribution for the quadrupole form factors, which are also small when compared with G_M^* [32,33].

However, it is well known that only the valence quark contributions are insufficient to describe the $\gamma N \rightarrow \Delta(1232)$ transition [1,31,43,45–48]. The pion cloud contributions, which a photon couples to the intermediate pion-baryon states, must also be included additionally to

the valence quark contributions [1,12,15,18,31,32,43]. Thus, the $\gamma N \rightarrow \Delta(1232)$ transition form factor G_M^* may be split into two contributions,

$$G_M^*(Q^2) = G_M^b(Q^2) + G_M^\pi(Q^2), \tag{1}$$

where G_M^b and G_M^π represent the contributions from the quark core (also denoted by "bare"), and those from the pion cloud, respectively. The above separation is justified if the pion is created by the baryon of a three-quark system, and not by a single quark inside the baryon. Also, according to the chiral perturbation theory, heavy meson loops are suppressed, and the processes with one pion loop are dominant in the low Q^2 region [49,50]. Thus, we restrict the pion-baryon intermediate states to the lowest order, namely, "one pion in the air" in the following.

With the decomposition of Eq. (1), we can separate the short-range contributions that are sensitive to the quark structure (G_M^b) [18], and those of the long-range which depend on the pion cloud (G_M^π). We note that the same decomposition Eq. (1) was also applied in several works [12,15,18,51–53].

To estimate the quark core contributions G_M^b, one needs a microscopic quark model of baryons. As for the pion cloud contributions G_M^π, one can use a long-range effective dynamics in the low Q^2 region based on chiral symmetry. According to chiral perturbation theory the two regimes cannot in general be disentangled [54]. That separation is possible only in a specific formalism, provided that the scale of the quark core is defined.

In the covariant spectator quark model $G_M^b(Q^2)$ was calculated for the $\gamma N \rightarrow \Delta(1232)$ transition by the processes in which a photon directly couples to the constituent quarks [31]. Here, the overlap integral between the nucleon and Δ scalar wave functions played an important role [31], as will be also discussed in Sec. III. The model for the $\Delta(1232)$ structure was calibrated by the core contributions of the Sato-Lee model by switching off the pion cloud effects [18]. Furthermore, the model was successfully able to reproduce the quenched lattice QCD data [55] for heavy pions, where the pion cloud effects are known to be small [33,35]. These facts give us some confidence that the valence quark contributions of the model are well under control.

To describe the $\gamma N \rightarrow \Delta(1600)$ transition, we use the same formalism which was successfully applied to study the $\gamma N \rightarrow \Delta(1232)$ transition [31–33,35] and $\Delta(1232)$ elastic form factors [36,37]. As the $\Delta(1600)$ resonance shares many common properties with the $\Delta(1232)$ resonance such as spin and isospin, it is reasonable to assume the $\Delta(1600)$ as the first radial excitation of the $\Delta(1232)$, and that it can also be described by an S-state approximation. Then, one can determine the $\Delta(1600)$ wave function completely by the orthogonality condition to that of the $\Delta(1232)$. Using the $\Delta(1600)$ wave function determined in this way and the nucleon wave function determined in the

previous study [29], we can estimate the valence quark contributions for the transition magnetic dipole form factor, G_M^b, for the $\gamma N \rightarrow \Delta(1600)$ transition. The detail will be given in next section.

On the other hand, the pion cloud contributions (G_M^π) for the $\gamma N \rightarrow \Delta(1232)$ transition in the spectator formalism was estimated using an effective parametrization [31]. The parametrization is consistent with the pion cloud contributions derived from the dynamical meson-baryon coupled-channel models of Sato-Lee [18], and Mainz-Taipei [12]. The relative contributions of the pion cloud (G_M^π/G_M^*) are simulated by a dipole form factor which suppresses the pion cloud contributions in the high Q^2 region.

To take account of the pion cloud contributions G_M^π in the $\gamma N \rightarrow \Delta(1600)$ transition, we must include more pion-baryon intermediate states than for the $\gamma N \rightarrow \Delta(1232)$ transition. The detailed discussions concerning the pion cloud effects are given in Sec. IV.

In the present work we adopt a hybrid approach to study the $\gamma N \rightarrow \Delta(1600)$ transition, which was successfully applied for the $\gamma N \rightarrow \Delta(1232)$ transition. This hybrid approach has the following advantages. It can explain why the bare contributions are insufficient to describe the electromagnetic transition form factors. Furthermore, it provides a simple parametrization for G_M^b that cannot be derived from usual dynamical coupled-channel models. Finally, it can also incorporate the pion cloud effects which is justified by dynamical coupled-channel models, and essential to describe the $\gamma N \rightarrow \Delta(1232)$ transition.

III. VALENCE QUARK CONTRIBUTIONS FOR THE $\gamma N \rightarrow \Delta$ TRANSITION

In the covariant spectator quark model a baryon is described as a system of three constituent quarks: one off-mass-shell quark free to interact with a electromagnetic field, and two on-shell quarks that act as an on-shell diquark with a mass m_D. In this formalism [29] the quark-diquark vertex is assumed to be zero at the singularity point of the three-quark propagator, and this corresponds to an effective description of confinement [29,56,57]. The nucleon and $\Delta(1232)$ states can be well approximated by a quark-diquark system with zero relative orbital angular momentum [29,31]. This S-state structure is sufficient to reproduce the nucleon elastic form factor data [29] and the dominant contributions for the $\gamma N \rightarrow \Delta(1232)$ transition [31]. We call this the S-state approach or S-state approximation hereafter.

A. Transition current

In the spectator quark model the electromagnetic current for a transition between an initial state Ψ_i and a final state Ψ_f is given by,

$$J^\mu = 3 \sum_\lambda \int_k \bar{\Psi}_f(P_+, k) j_I^\mu \Psi_i(P_-, k), \qquad (2)$$

where k is the diquark on-shell momentum, $\int_k \equiv \int \frac{d^3k}{2E_D(2\pi)^3}$ with E_D the diquark on-shell energy, P_- (P_+) is the initial (final) momentum, $q = P_+ - P_-$, λ is the diquark polarization $(0, \pm 1)$ and j_I^μ the quark current. The factor 3 comes from the symmetrization in the quark flavor (see Refs. [29,38,39] for details). In the above, the diquark polarization and the baryon spin projection indices are suppressed.

The constituent quark current can be decomposed by

$$j_I^\mu = j_1(Q^2)\left(\gamma^\mu - \frac{\not{q}q^\mu}{q^2}\right) + j_2(Q^2)\frac{i\sigma^{\mu\nu}q_\nu}{2M}, \qquad (3)$$

where M is the nucleon mass. The Dirac (j_1) and Pauli (j_2) quark form factors in the above are also decomposed into the isoscalar and isovector components:

$$j_i(Q^2) = \frac{1}{6}f_{i+}(Q^2) + \frac{1}{2}f_{i-}(Q^2)\tau_3, \qquad (i = 1, 2). \quad (4)$$

The quark form factors $f_{i\pm}$ are normalized to $f_{1\pm}(0) = 1$ and $f_{2\pm}(0) = \kappa_\pm$ (isoscalar and isovector quark anomalous moments). Their explicit expressions are given in Refs. [29,31,32,38,39].

B. Baryon wave functions

In the S-state approach the nucleon wave function, $\Psi_N(P, k)$, with P (k) being the nucleon (diquark) momentum, can be written as [29],

$$\Psi_N(P, k) = \frac{1}{\sqrt{2}}[\phi_I^0 \phi_S^0 + \phi_I^1 \phi_S^1]\psi_N(P, k), \qquad (5)$$

where $\phi_{I,S}^{0,1}$ represents isospin (I) or spin (S) states corresponding to the total magnitude of either 0 or 1 in the diquark configuration [29]. In Eq. (5), $\psi_N(P, k)$ is the nucleon scalar wave function to be specified later.

A generic Δ state (spin 3/2) with mass M_Δ is represented in the S-state approach, as proposed in Ref. [31],

$$\Psi_\Delta(P, k) = -\psi_\Delta(P, k)\tilde{\phi}_I^1 \varepsilon_P^{\beta *} u_\beta(P), \qquad (6)$$

where P (k) is the total (diquark) momentum, u_β the Rarita-Schwinger vector-spinor, ε_P the polarization vector in the fixed-axis representation [30], $\tilde{\phi}_I^1$ is the isospin state associated with the isospin-1 diquark in a spin 3/2 system [31] and $\psi_\Delta(P, k)$ is a scalar wave function also to be specified later. In the above, both nucleon and Δ wave functions satisfy the Dirac equation with respective masses [29,31,32].

C. Form factors

The $\gamma N \rightarrow \Delta$ transition, between a nucleon and a Δ in S-states, is characterized by a magnetic dipole form factor,

$$G_M^b(Q^2) = \frac{8M}{3\sqrt{3}(M_\Delta + M)}f_v(Q^2)\mathcal{I}_{\Delta N}(Q^2), \qquad (7)$$

with

$$f_v(Q^2) = f_{1-}(Q^2) + \frac{M_\Delta + M}{2M} f_{2-}(Q^2). \qquad (8)$$

In Eq. (7), $I_{\Delta N}(Q^2)$ is the overlap integral between the Δ and nucleon S-state scalar wave functions:

$$I_{\Delta N}(Q^2) = \int_k \psi_\Delta^*(P_+, k)\psi_N(P_-, k). \qquad (9)$$

Equations (7)–(9) hold for a generic transition between a spin $1/2$ (N) and a spin $3/2$ (Δ) baryons described by the S-state approximation.

D. Model for the scalar wave functions

In the following we use notations, Δ, Δ^* and N^* for $\Delta(1232)$, $\Delta(1600)$ and $N(1440)$, respectively, whenever convenient.

To describe the momentum distribution of the quark-diquark system in a baryon B, we introduce a scalar wave function ψ_B, which depends on the relative angular momentum and the radial excitation of the system. As the baryon and the diquark are on-shell in the covariant spectator model, the scalar wave function ψ_B can be written as a function of $(P - k)^2$ [29]. The dependence on these momenta can be made in terms of the dimensionless variable [29],

$$\chi_B = \frac{(M_B - m_D)^2 - (P - k)^2}{M_B m_D}, \qquad (10)$$

where M_B is the baryon mass ($B = N, N^*, \Delta, \Delta^*$).

The nucleon scalar wave function ψ_N is defined by [29]

$$\psi_N(P, k) = \frac{N_0}{m_D(\beta_1 + \chi_N)(\beta_2 + \chi_N)}, \qquad (11)$$

where χ_N is obtained by inserting $M_B = M$ in Eq. (10), and N_0 the normalization constant [29]. In a parametrization where $\beta_2 > \beta_1$, β_1 is associated with the long-range physics, while β_2 the short-range physics.

As for the Δ, we use the form proposed in Ref. [31] based on an S-wave ground state configuration,

$$\psi_\Delta(P, k) = \frac{N_1}{m_D(\alpha_1 + \chi_\Delta)(\alpha_2 + \chi_\Delta)^2}, \qquad (12)$$

where N_1 is the normalization constant, and α_1 and α_2 are the parameters which control the momentum ranges with $\alpha_2 > \alpha_1$. The α_1 is associated with the long-range physics in the Δ system [31]. Note that the difference in the form of ψ_Δ wave function from that of the nucleon in Eq. (11). Namely, an extra power in ψ_Δ exists, and this is preferred by the magnetic dipole form factor (G_M^*) data in the $\gamma N \to \Delta(1232)$ transition [31,32]. The description of the $\gamma N \to \Delta(1232)$ transition can be improved with the inclusion of D-states, which induce also nonzero G_E^* and G_C^* form factors. But the inclusion of D-states requires extra parameters [31,33]. In that case (with D-states) the two

parameters α_1, α_2 are degenerate [33]. In this study we do not include any D-states, since the S-states are sufficient to describe well the $\gamma N \to \Delta(1232)$ transition, with only two parameters in the valence quark sector.

The quality of the present model description for the $\gamma N \to \Delta(1232)$ can be understood by comparing with the G_M^* data, or with the helicity amplitudes $A_{1/2}$ and $A_{3/2}$, which will be shown in in Sec. V.

For the Δ^* wave function we assume the same structure as that of the Δ presented in Eq. (6), except for the scalar wave function. To represent Δ^* as the first radial excitation of Δ, we write the Δ^* scalar wave function in the form,

$$\psi_{\Delta^*}(P, k) = N_2 \frac{\alpha_4 - \chi_{\Delta^*}}{(\alpha_3 + \chi_{\Delta^*})} \frac{1}{m_D(\alpha_1 + \chi_{\Delta^*})(\alpha_2 + \chi_{\Delta^*})^2}, \qquad (13)$$

where $\alpha_3 = \alpha_1$ will be assumed later, and α_4 is a new parameter to be fixed by the orthogonality condition between the Δ and Δ^* states. The normalization constant N_2 will be fixed by $\int_k |\psi_{\Delta^*}|^2 = 1$ at $Q^2 = 0$, similarly to the nucleon and Δ cases [29,31,32,36,37].

The extra factor $\frac{\alpha_4 - \chi_R}{(\alpha_3 + \chi_R)}$ in Eq. (13) is motivated by the wave functions obtained in a harmonic-oscillator potential model for the three-quark system [21,58–60]. A similar form was also applied for describing the Roper resonance [34].

In the numerical calculation we will use $\alpha_3 = \alpha_1$, assuming that the Δ and Δ^* are described by the same short-range structure. The difference between the Δ and Δ^* systems appear in the structure, $\alpha_4 - \chi_{\Delta^*}$, scaled by the long-range factor, $\alpha_3 + \chi_{\Delta^*}$. Thus, α_4 is the only parameter characteristic in the Δ^* scalar wave function. With the scalar wave functions for the Δ and Δ^* respectively, Eqs. (12) and (13), there is no guaranty that the orthogonality condition is satisfied for an arbitrary value of α_4. The value of α_4 will be determined by imposing the orthogonality condition for the Δ and Δ^* states. This will be explained in next section. Thus, to write down the Δ^* wave function, no extra parameter is necessary, since the parameters α_1 and α_2 have already been fixed by the Δ wave function [31].

E. Orthogonality condition

The orthogonality between the Δ^* and Δ states is ensured if the overlap integral of the Δ^* and Δ wave functions vanishes for $Q^2 = 0$. This leads to

$$\int_k \psi_{\Delta^*}^*(P_{\Delta^*}, k)\psi_\Delta(P_\Delta, k)\big|_{Q^2=0} = 0, \qquad (14)$$

the orthogonality between the scalar wave functions. In the Δ^* rest frame the momenta of the Δ and Δ^* corresponding to $Q^2 = 0$ are

$$P_\Delta = \left(\frac{M_{\Delta^*}^2 + M_\Delta^2}{2M_\Delta}, 0, 0, -\frac{M_{\Delta^*}^2 - M_\Delta^2}{2M_\Delta}\right),$$

$$P_{\Delta^*} = (M_{\Delta^*}, 0, 0, 0). \tag{15}$$

The condition Eq. (14) may be regarded as the simplest generalization of the nonrelativistic orthogonality condition, where equal mass states are orthogonal when $\mathbf{q}^2 = -Q^2 = 0$. See Ref. [34] for more details, where the same orthogonality condition was applied for the nucleon and Roper state.

IV. PION CLOUD

In the electromagnetic interactions with baryons there are two main contributions: a photon couples to an individual quark, which we will call core or "bare," and a photon couples to the meson-baryon intermediate states, which we will call meson cloud. As mentioned already the intermediate states, where the meson is a pion, are dominant. In general, contributions from the pion cloud decrease with increasing Q^2 but can be significant at low Q^2. Among all the processes, one pion "in the air" are the most important according to chiral perturbation theory [49,50,54]. In the lowest order the dominant processes for the $\gamma B \to B^*$ transition are shown in Fig. 1: (a) a photon couples to the pion, and (b) a photon couples to the baryon (vertex correction). The relative contributions of the processes (a) and (b) are dependent on the systems and observables in consideration. We note that the diagram (b) represents two kinds of interactions: (b1) a photon interacts with the baryon charge (electric), and (b2) a photon interacts with the baryon anomalous magnetic moment (magnetic).

In elastic reactions both contributions (a) and (b1) must be included consistently for the electric form factor to satisfy the baryon charge conservation (see e.g., Ref. [39]). However, in inelastic transitions like the $\gamma N \to \Delta$ transition, the dominant contributions are from the magnetic transition form factor. When there are two contributions (b1) and (b2), (b1) is dominant in general. Also contributions from (a) dominate in general over (b). This is justified by chiral perturbation theory. A diagram with two baryon propagators with one pion loop is suppressed
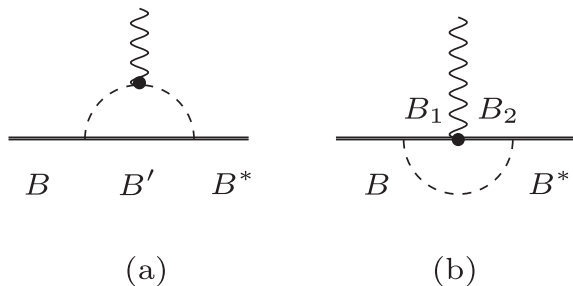
compared to a diagram with two pion propagators [61]. Furthermore, in the study of the octet magnetic moments with the same spectator formalism, it was indeed found that the contributions from the diagram (a) are dominant [39]. The contributions from the diagram (b) amount to at most 9% of the diagram (a) for the magnetic moments except for the Λ baryon case.[1] Diagram (a) is also dominant in the decuplet baryon magnetic moments [62].

Thus, in the present covariant spectator formalism, we can assume the diagram (a) is dominant for the magnetic form factor due to the pion cloud, and may neglect the diagram (b) within an ambiguity of about 10%. Then, we will only focus on the processes represented by the diagram (a), a photon couples to the pion.

To describe the effect of the pion cloud in the $\gamma N \to \Delta$ and $\gamma N \to \Delta^*$ transitions, one needs a microscopic description for the pion-baryon interactions as well as the photon-pion interactions. For this, treating the pion as a pointlike particle, we use the formalism of the cloudy bag model (CBM) [63,64]. In CBM, a pion couples to a baryon, not to a quark nor exchanged among the quarks inside the baryon. This is exactly the same approach as that of the covariant spectator constituent quark model used in the present study.[2] CBM is particularly useful to describe the pion cloud dressing. For the typical bag radius the one pion "in the air" processes are dominant and the interaction can be treated perturbatively [65–67]. We can obtain various pion-baryon coupling constant ratios, and carry out intermediate state spin and isospin sums by the formalism based on CBM. It provides a systematic method to calculate these ingredients based on a SU(6) quark model. Thus, the amplitudes associated with the diagram (a) are represented in terms of the coupling constants, a coefficient comes from the intermediate spin and isospin sums, and a scalar integral involving the quark wave functions, all can be estimated based on the formalism of CBM. In the end we replace the respective contributions due to various intermediate states by an effective covariant parametrization. The formalism can be used to relate the pion cloud contributions associated with different pion-baryon intermediate states. We note that the coupling constants used in the present study are not obtained from CBM, but are calculated from the decay branches of the resonances using effective Lagrangians. Only the relevant coupling constant ratios are calculated based on the CBM formalism.

For the $\gamma N \to \Delta(1232)$ reaction, the pion cloud can contribute for the form factors G_M^*, G_E^* and G_C^* in the

FIG. 1. Electromagnetic transition, $\gamma B \to B^*$ with one pion loop (pion cloud) through the intermediate states.

---

[1]The Λ baryon case is special, since it has a small bare magnetic moment. It has no contributions from the diagrams (a) but has only from the diagram (b), by the anomalous coupling of the intermediate state Σ baryons, Σ^+, Σ^0 and Σ^- [39].

[2]Note that in the spectator constituent quark model the processes where the pion is created and absorbed by the same quark are already included in the constituent quark structure through the quark electromagnetic form factors.

spectator quark model [32,33]. Although the pion cloud contributions for the quadrupole form factors can be appreciable compared to the valence quark contributions (from D-states), these contributions are all small compared to G_M^* [32,33]. Thus, we consider only the pion cloud contributions for the magnetic dipole form factor G_M^* for the $\gamma N \to \Delta(1232)$ and $\gamma N \to \Delta(1600)$ reactions.

In the following we first discuss the pion cloud contributions for the $\gamma N \to \Delta$ transition, and then discuss the $\gamma N \to \Delta^*$ transition. Finally, we make a connection for the pion cloud contributions between the two transitions.

A. $\gamma N \to \Delta(1232)$ transition

In the description of the $\gamma N \to \Delta$ transition, the pion cloud contributions for G_M^* can be simulated by the parametrization [31,32],

$$G_M^\pi(Q^2) = \lambda_\pi \left(\frac{\Lambda_\pi^2}{\Lambda_\pi^2 + Q^2}\right)^2 (3G_D), \qquad (16)$$

where $G_D = (1 + Q^2/0.71)^{-2}$ (Q^2 in GeV^2) is the nucleon dipole form factor. Here, the parameter λ_π gives the pion cloud contribution strength, and Λ_π is a momentum cutoff parameter. The simple parametrization of Eq. (16) can describe well the main feature of the pion cloud contributions consistently with the more sophisticated dynamical coupled-channel models [12,18]. With the parametrization Eq. (16) we get a significant contribution for the pion cloud contributions near $Q^2 = 0$ (46.4% at $Q^2 = 0$, using the parametrization of Ref. [31]), and a fast falloff with increasing Q^2. The falloff of the pion cloud contributions is controlled by Λ_π^2 ($\simeq 1.22$ GeV^2) [31]. This consistently leads to the dominance of the valence quark contributions in the region $Q^2 > 3$ GeV^2.

Using the CBM [64,66,68–73] framework[3] we can write down the strength of the photon-pion coupling diagram (a) in Fig. 1, in the low Q^2 region as follows,

$$\lambda_\pi = -2\sqrt{\frac{2}{3}}\mathcal{K}f_{\pi NN}f_{\pi N\Delta}\hat{\mathcal{C}}_{N\Delta} - 10\sqrt{\frac{2}{3}}\mathcal{K}f_{\pi N\Delta}f_{\pi\Delta\Delta}\hat{\mathcal{C}}_{\Delta\Delta}, \qquad (17)$$

where $\mathcal{K}$ is a generic constant associated with the interaction and the angular integration. The factor $\hat{\mathcal{C}}_{BB'}$ represents the ratio,

$$\hat{\mathcal{C}}_{BB'} = \frac{\mathcal{C}_{BB'}(Q^2)}{\mathcal{C}_{N\Delta}(Q^2)}, \qquad (18)$$

where $\mathcal{C}_{BB'}(Q^2)$ is a scalar integral that corresponds to the diagram with the intermediate baryon B and the final baryon B' states, and $\mathcal{C}_{N\Delta}(Q^2)$ is the case of $B = N$ and $B' = \Delta$. The integrals $\mathcal{C}_{BB'}$ in CBM depend on the pion-baryon form factor [63,64,66].

---

[3]In our notation $f_{\pi N\Delta}$ corresponds to $f_{\Delta N}$ in CBM [64,66],

In Eq. (17) the first and the second terms correspond, respectively, to the intermediate N and Δ states for the diagram (a) in Fig. 1. In the ratio in Eq. (18) we expect that the Q^2 dependence largely cancels out, and may regard the ratio as a constant in the low Q^2 region, where the pion cloud is dominant.

The coupling constant $f_{\pi BB'}$ may be calculated using effective Lagrangians. In the present study, we use the relative strength to $f_{\pi NN} = 1$ ($f_{\pi NN}^2/4\pi = 0.08$), since what matters is the relative sign and ratio to the $f_{\pi NN}$, as will be discussed later.

B. $\gamma N \to \Delta(1600)$ transition

To extend the description of the pion cloud contributions from the $\gamma N \to \Delta(1232)$ transition to the $\gamma N \to \Delta(1600)$ transition, we include the dominant intermediate states. In the processes with intermediate baryon state B, $\gamma N \to \pi B \to \Delta^*$, we include the intermediate states, πN, $\pi N(1440)$ and $\pi\Delta$ as observed by the $\Delta(1600)$ decay [20]. In addition, the $\pi\Delta(1600)$ intermediate state is also included. The strength of the pion cloud contributions from these intermediate states can be calculated based on the CBM formalism. In the following we denote the contributions from the processes, $\gamma N \to \pi B \to \Delta(1600)$ with $B = N$, Δ, $N(1440)$, $\Delta(1600)$, by λ_π^B. The explicit expressions are given by

$$\lambda_\pi^N = -2\sqrt{\frac{2}{3}}\mathcal{K}f_{\pi NN}f_{\pi N\Delta^*}\hat{\mathcal{C}}_{N\Delta^*},$$

$$\lambda_\pi^{N^*} = -2\sqrt{\frac{2}{3}}\mathcal{K}f_{\pi NN^*}f_{\pi N^*\Delta^*}\hat{\mathcal{C}}_{N^*\Delta^*},$$

$$\lambda_\pi^\Delta = -10\sqrt{\frac{2}{3}}\mathcal{K}f_{\pi N\Delta}f_{\pi\Delta\Delta^*}\hat{\mathcal{C}}_{\Delta\Delta^*}, \qquad (19)$$

$$\lambda_\pi^{\Delta^*} = -10\sqrt{\frac{2}{3}}\mathcal{K}f_{\pi N\Delta^*}f_{\pi\Delta^*\Delta^*}\hat{\mathcal{C}}_{\Delta^*\Delta^*},$$

where, $\hat{\mathcal{C}}_{BB'}$ is defined by Eq. (18).

With this procedure, we have reduced the estimate of the pion cloud contributions for the $\gamma N \to \Delta(1600)$ to the evaluation of the factor,

$$\lambda_\pi' = \lambda_\pi^N + \lambda_\pi^{N^*} + \lambda_\pi^\Delta + \lambda_\pi^{\Delta^*}. \qquad (20)$$

Because of the similarity between the $\gamma N \to \pi B \to \Delta(1600)$ and $\gamma N \to \pi B \to \Delta(1232)$ processes, one can expect that λ_π' can also be well approximated by a constant, and the pion cloud contributions can be parameterized by the same form as that for the $\gamma N \to \Delta(1232)$ transition. Thus, as in Eq. (16), pion cloud contributions for the G_M^* form factor in the $\gamma N \to \pi B \to \Delta(1600)$ transition may be given by

$$G_M^\pi(Q^2) = \lambda_\pi' \left(\frac{\Lambda_\pi^2}{\Lambda_\pi^2 + Q^2}\right)^2 (3G_D). \qquad (21)$$

C. Relation between the pion cloud contributions in the $\gamma N \to \Delta(1232)$ and $\gamma N \to \Delta(1600)$ reactions

It may be a little crude, but as an exploratory study, we neglect the mass differences of the baryons involved, and using the formalism based on CBM [64,66,68–70]. As a consequence we can write $\hat{\mathcal{C}}_{\Delta\Delta} = \hat{\mathcal{C}}_{N\Delta}$. Using the relation from CBM, $f_{\pi NN} = f_{\pi\Delta\Delta}$, together with the value $f_{\pi NN} = 1$, we can rewrite Eq. (17) as

$$\lambda_\pi = -12\sqrt{\frac{2}{3}} \mathcal{K} f_{\pi N\Delta} \hat{\mathcal{C}}_{N\Delta}. \tag{22}$$

In the above, the index $N\Delta$ in $\hat{\mathcal{C}}_{N\Delta}$ is explicit for a reminder but note that $\hat{\mathcal{C}}_{N\Delta} = \hat{\mathcal{C}}_{NN}$. With the same approximation for Eq. (19), namely, $\hat{\mathcal{C}}_{BB'} \to \hat{\mathcal{C}}_{N\Delta}$, and together with the result of Eq. (22), we get the ratios:

$$\begin{aligned}
\frac{\lambda_\pi^N}{\lambda_\pi} &= \frac{1}{6} \frac{f_{\pi N\Delta^*}}{f_{\pi N\Delta}}, \\
\frac{\lambda_\pi^{N^*}}{\lambda_\pi} &= \frac{1}{6} f_{\pi NN^*} \frac{f_{\pi N\Delta^*}}{f_{\pi N\Delta}}, \\
\frac{\lambda_\pi^\Delta}{\lambda_\pi} &= \frac{5}{6} f_{\pi N\Delta} \frac{f_{\pi\Delta\Delta^*}}{f_{\pi N\Delta}} = \frac{5}{6} f_{\pi\Delta\Delta^*}, \\
\frac{\lambda_\pi^{\Delta^*}}{\lambda_\pi} &= \frac{5}{6} \frac{f_{\pi N\Delta^*}}{f_{\pi N\Delta}}.
\end{aligned} \tag{23}$$

The coupling constants, $f_{\pi BB'}$, can be calculated from the $B' \to \pi B$ branching ratios with some effective Lagrangians at the hadronic level. This will be discussed in the next section.

D. Estimates of the coupling constants $f_{\pi BB'}$

The interaction Lagrangians and definitions of the coupling constants $\pi BB'$ relevant in this study are given in the Appendix. Based on these interaction Lagrangians and decay rate expressions, we obtain the absolute values of the coupling constants. The data used for the calculation, extracted from the Particle Data Group [20], are summarized in Table I. To determine the relative signs for the

coupling constants we follow some quark models [4,63,64,74]. For the πNN constant, we use the positive value $f_{\pi NN} = 1$ (or $f_{\pi NN}^2/4\pi = 0.08$), since what matters is the relative sign and strength to $f_{\pi NN}$. For the signs of the coupling constants, $f_{\pi NN(1440)}$, $f_{\pi N\Delta}$ and $f_{\pi N\Delta(1600)}$, we take the same sign as that of the $f_{\pi NN}$ as suggested by the quark model results [74]. For a detailed discussion about the sign of $f_{\pi NN(1440)}$ see also Ref. [4]. Then, the relative signs undetermined are those for $f_{\pi\Delta\Delta(1600)}$ and $f_{\pi N(1440)\Delta(1600)}$. Since Δ and $\Delta(1600)$ differ only in radial excitations (and thus mass), we assume the same relative sign for these coupling constants. The same argument also holds for the case where N is replaced by $N(1440)$. As a result all the coupling constants relevant in this study are assigned to the same sign as that of the $f_{\pi NN}$. The coupling constants calculated in these manners, are presented in Table I. The values obtained in the present study are similar to those obtained in Refs. [14,74].

V. HELICITY AMPLITUDES AND FORM FACTORS

As already mentioned, the description of the $\gamma N \to \Delta$ transition is characterized by the three independent multipole form factors, G_M^*, G_E^* and G_C^* [40]. These form factors are exclusive functions of the four-momentum transfer squared Q^2 and frame independent. The physical properties of the $\gamma N \to \Delta$ transition are usually expressed in terms of the transition amplitudes in a particular frame. As there are amplitudes associated with any photon polarization including the longitudinal polarization, there are three independent transition amplitudes, $A_{1/2}$, $A_{3/2}$ and $S_{1/2}$ [4,59]. The helicity amplitudes for the transitions, $\gamma N \to \Delta$ or $\gamma N \to \Delta(1600)$ at the final particle rest frame, can be related with the form factors by [21]:

$$G_M^*(Q^2) = -F(Q^2)[\sqrt{3} A_{3/2}(Q^2) + A_{1/2}(Q^2)], \tag{24}$$

$$G_E^*(Q^2) = -F(Q^2)\left[\frac{1}{\sqrt{3}} A_{3/2}(Q^2) - A_{1/2}(Q^2)\right]. \tag{25}$$

In the above the factor $F(Q^2)$ is given by

TABLE I. Data for resonances from PDG [20], and the coupling constants calculated. For $f_{\pi NN}$, we use $f_{\pi NN} = 1$ ($f_{\pi NN}^2/4\pi = 0.08$) and the relation based on CBM [63,64,68–70], $f_{\pi NN} = f_{\pi\Delta\Delta} = f_{\pi\Delta^*\Delta^*}$. For the branching ratios, we take an average weighted by the error of the selected results from PDG. Errors in coupling constants are estimated using Gaussian quadrature.

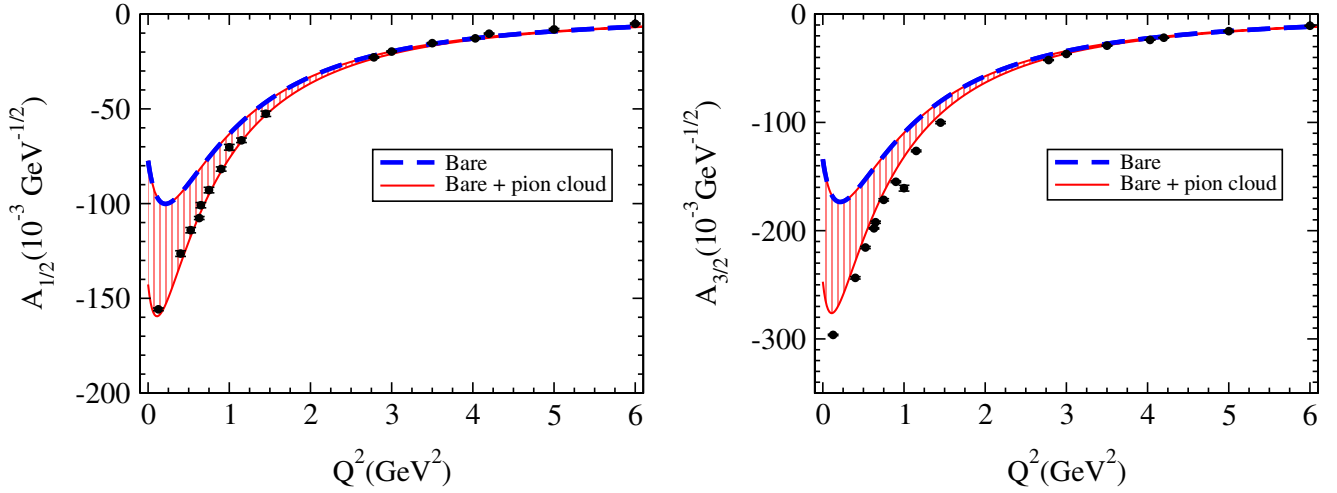| Decay	Γ (MeV)	BR	$f_{\pi NB'}$
$N(1440) \to \pi N$	300 ± 100	0.706 ± 0.014	0.367 ± 0.061
$\Delta \to \pi N$	118 ± 2	1.00	2.160 ± 0.018
$\Delta(1600) \to \pi N$	350 ± 100	0.153 ± 0.019	0.477 ± 0.074
Decay	Γ (MeV)	BR	$f_{\pi B\Delta^*}$
$\Delta(1600) \to \pi\Delta$	350 ± 100	0.590 ± 0.100	0.653 ± 0.108
$\Delta(1600) \to \pi N(1440)$	350 ± 100	0.130 ± 0.040	6.330 ± 1.329

FIG. 2 (color online). Helicity amplitudes calculated for the $\gamma N \rightarrow \Delta(1232)$ transition in the S-state approach, with and without the pion cloud contributions. Data are taken from the MAID analysis [2].

$$F(Q^2) = \frac{1}{e} \sqrt{\frac{M(M_\Delta^2 - M^2)}{2[(M_\Delta - M)^2 + Q^2]}} \frac{2M}{M_\Delta + M}, \qquad (26)$$

where $e = \sqrt{4\pi\alpha}$ is the magnitude of the electron charge, with $\alpha = 1/137.036$ the fine-structure constant. There is an extra relation between the transverse amplitude $S_{1/2}$ and G_C^*, but we omit it since it is irrelevant in the present study.

In a model with an S-state approach for the nucleon and Δ and the pion cloud contributes only for G_M^*, G_M^* is dominant, and one has $G_E^* \equiv 0$, $G_C^* \equiv 0$ [31,32]. In these conditions with $G_E^*(Q^2) = 0$ for an arbitrary Q^2, we get

$$A_{3/2}(Q^2) = -\frac{\sqrt{3}}{2F(Q^2)} G_M^*(Q^2), \qquad (27)$$

$$A_{1/2}(Q^2) = -\frac{1}{2F(Q^2)} G_M^*(Q^2). \qquad (28)$$

Thus, we can write the helicity amplitudes $A_{1/2}$ and $A_{3/2}$ in terms of G_M^* for an arbitrary Q^2. As for the transverse amplitude $S_{1/2}$, which is proportional to G_C^*, one has $S_{1/2} \equiv 0$.

The helicity amplitudes $A_{1/2}$ and $A_{3/2}$ for the $\gamma N \rightarrow \Delta(1232)$ in the S-state approach, as well as the contributions from the quark core, are presented in Fig. 2. From the figure, one can see that the S-state approximation plus pion cloud dressing (for G_M^*) reproduces well the data for $\gamma N \rightarrow \Delta(1232)$ transition. Encouraged by this, we will use the same approximation for the $\gamma N \rightarrow \Delta(1600)$ transition. The S-state approach will be tested in next section.

VI. RESULTS

In this section we present numerical results for the form factors and helicity amplitudes. Because of the approximation used in this exploratory study, it holds that $G_E^* = 0$

and $G_C^* = 0$ for all Q^2. Thus, we have nonzero results only for G_M^*. The electric (E2) and Coulomb (C2) quadrupole form factors both vanish, as well as the ratios, E2/M1 and C2/M1. We start by the case $Q^2 = 0$ and compare the results with the available experimental data. Next we discuss the Q^2 dependence of the form factors and make some predictions.

The experimental information for the $\gamma N \rightarrow \Delta(1600)$ transition is restricted to the helicity amplitudes $A_{1/2}$ and $A_{3/2}$ measured in the $\Delta(1600)$ rest frame at the photon point ($Q^2 = 0$). This is collected in Ref. [20] by PDG. Particle Data Group selected three results: Awaji, Crawford [75] and Arndt [76]. The result of Awaji has a large uncertainty. The results from PDG together with the result calculated for $G_M^*(0)$ and $G_E^*(0)$ by Eqs. (24) and (25) are presented in the following section.

A. Analysis in the limit $Q^2 = 0$

We discuss first the contributions from the valence quarks (G_M^b). In the S-state approach G_M^b is given by Eq. (7). With the scalar wave function Eq. (12), and the mass M_Δ, we get the result for the $\gamma N \rightarrow \Delta(1232)$ transition. Similarly, with the scalar wave function Eq. (13), and M_Δ replaced by M_{Δ^*}, we can get the result for the $\gamma N \rightarrow \Delta(1600)$ transition. Note that it is the scalar wave function ψ_Δ or ψ_{Δ^*} that characterizes the radial state (ground state or first radial excited state). We adopt model II in Ref. [31]: $\alpha_1 = 0.290$ and $\alpha_2 = 0.393$. The normalization constant is $N_1 = 2.95$. The Δ^* wave function is determined by the scalar wave function Eq. (13) with $\alpha_3 = \alpha_1$, where α_1 is the parameter associated with the long-range scale. The unknown parameter α_4 is determined by the orthogonality condition Eq. (14), which gives $\alpha_4 = -0.0353$. The corresponding normalization constant for the Δ^* scalar wave function is $N_2 = 7.27$. The parame-

TABLE II.   Results for the coupling constants and λ_π^B [$B = N$, $N(1440)$, Δ, $\Delta(1600)$]. The total contribution of the pion cloud is given by the sum of λ_π^B, which amounts to $0.9442\lambda_\pi$, where $\lambda_\pi = 0.464$ [31]. The uncertainty in the final result (Total) is obtained by adding the errors in Gaussian quadrature.

$\gamma N \rightarrow \pi B \rightarrow \Delta(1600)$	$f_{\pi NB}$	$f_{\pi B\Delta(1660)}$	$\lambda_\pi^B/\lambda_\pi$
$\gamma N \rightarrow \pi N \rightarrow \Delta(1600)$	1.000	0.477	0.0368 ± 0.0057
$\gamma N \rightarrow \pi N(1440) \rightarrow \Delta(1600)$	0.361	6.330	0.1791 ± 0.0481
$\gamma N \rightarrow \pi \Delta \rightarrow \Delta(1600)$	2.160	0.653	0.5441 ± 0.0904
$\gamma N \rightarrow \pi \Delta(1600) \rightarrow \Delta(1600)$	0.477	1.000	0.1842 ± 0.0287
Total			0.9442 ± 0.1065

ters associated with the nucleon scalar wave function are given by model II of Ref. [29]. With these parameters fixed, the overlap integral between the Δ^* and nucleon scalar wave function at $Q^2 = 0$ given by Eq. (9) with Δ replaced by Δ^*, is calculated:

$$\mathcal{I}_{\Delta^*N}(0) = -0.564. \tag{29}$$

Then, the contributions from the valence quarks (bare) for the magnetic dipole form factor at $Q^2 = 0$ of Eq. (7) result to

$$G_M^b(0) = -1.113. \tag{30}$$

Thus, the valence quark core contributions underestimate largely the experimental values and differ in sign from the data shown in Table III. We recall that in the present approach $G_E^* \equiv 0$.

Now, we turn our discussion to the pion cloud contributions. The pion cloud contributions for the transition magnetic form factor are estimated by Eq. (21). The coefficient λ_π' can be obtained by Eqs. (20) and (23). This includes contributions from the dominant intermediate baryon states, N, $N(1440)$, Δ, $\Delta(1600)$. These contributions depend on the $\pi BB'$ coupling constants. The coupling constants calculated from experimental data [20] are presented in Table I. Using these values we calculate λ_π', and each intermediate state contribution is listed in Table II. Then, we get the total contribution for the pion cloud, relative to those of the $\gamma N \rightarrow \Delta(1232)$:

$$\frac{\lambda_\pi'}{\lambda_\pi} = 0.944 \pm 0.107. \tag{31}$$

Once λ_π' is fixed, the pion cloud contributions for $G_M^\pi(0)$ are determined by Eq. (21) with $3G_D(0) = 3$:

$$G_M^\pi(0) = \frac{\lambda_\pi'}{\lambda_\pi}(3\lambda_\pi) = 1.314 \pm 0.148. \tag{32}$$

Adding the valence quark contributions and the pion cloud contributions, Eqs. (30) and (32), respectively, we get

$$G_M^*(0) = 0.202 \pm 0.131. \tag{33}$$

This result is compared with experimental data in Table III. The more accurate data available [75,76] supports the S-state approximation, and the consequent G_M^* dominance. The corresponding results for the helicity amplitudes, $A_{1/2}(0)$ and $A_{3/2}(0)$, are also presented in Table III.

B. Q^2 dependence of G_M^*

In our model the magnetic dipole form factor $G_M^*(Q^2)$ is given by the sum of $G_M^b(Q^2)$ and $G_M^\pi(Q^2)$. The valence quark contributions are given by Eq. (7), which includes the isovector factor $f_v(Q^2)$ and the Q^2 dependent overlap integral $\mathcal{I}_{\Delta^*N}(Q^2)$ between the Δ^* and nucleon scalar wave functions [see Eqs. (8) and (9)]. The Q^2 dependence of G_M^* is shown in Fig. 3. As for the pion cloud contributions G_M^π, these are determined by Eq. (21), once the coefficient λ_π' is known. The band in Fig. 3 shows the uncertainty in the estimate of the coupling $f_{\pi BB'}$ from the data listed in Table I.

Each pion cloud contribution due to the different intermediate states, N, $N^*\Delta$, Δ^*, is shown in Fig. 4, in an accumulative manner. As the pion cloud contributions from the different intermediated states are added one by one, the result for $G_M^*(0)$ approaches to the experimental data points accordingly. In Fig. 4, uncertainties in the pion cloud contributions are not shown for clarity. In the figure one can see that the $\pi\Delta$ intermediate state gives the

TABLE III.   Results at $Q^2 = 0$ compared with the selected data from PDG [20]. $G_E^* = 0$ is the consequence of the S-state approximation.

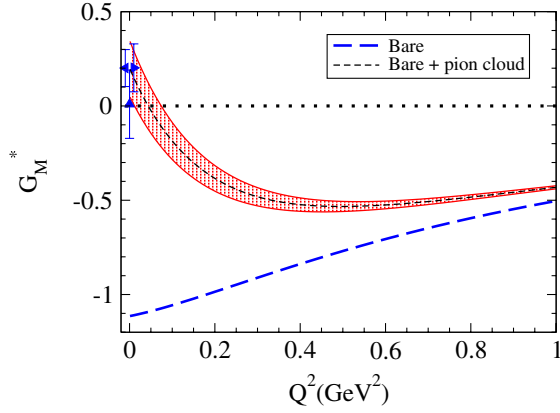|	$A_{1/2}(0)$ (GeV$^{-1/2}$)	$A_{3/2}(0)$ (GeV$^{-1/2}$)	$G_M^*(0)$	$G_E^*(0)$
Awaji 1981 [20]	-0.046 ± 0.013	$+0.025 \pm 0.031$	0.009 ± 0.181	-0.198 ± 0.073
Crawford 1983 [75]	-0.039 ± 0.030	-0.013 ± 0.014	0.202 ± 0.127	-0.103 ± 0.102
Arndt 1996 [76]	-0.018 ± 0.015	-0.025 ± 0.015	0.201 ± 0.098	-0.012 ± 0.057
Model	-0.0154 ± 0.0113	-0.0266 ± 0.0196	0.202 ± 0.148	0.000

FIG. 3 (color online). $\gamma N \to \Delta(1600)$ magnetic dipole form factor.

FIG. 5 (color online). Absolute values of the bare and the pion cloud contributions for the $\gamma N \to \Delta(1600)$ transition magnetic form factor.

dominant contribution. According to the values in Table II, the $\pi\Delta$ intermediate state contribution is about 48–67% of the total pion cloud contribution. The contributions from the πN^* and $\pi\Delta^*$ intermediate states amount to about 33–44% of the total pion cloud contribution. Figure 4 shows also a faster falloff of the pion cloud contributions with increasing Q^2, compared to the Q^2 dependence of the quark core. This can be better seen in Fig. 5, where absolute values of bare and pion cloud contributions are compared. In the same figure one can also see the pion cloud contributions are dominant near $Q^2 = 0$, while the bare (quark core) contributions (G_M^b) become dominant in the region $Q^2 > 0.5$ GeV^2.

C. Q^2 dependence of $A_{1/2}$ and $A_{3/2}$

Q^2 dependence of the helicity amplitudes, $A_{1/2}(Q^2)$ and $A_{3/2}(Q^2)$, can be obtained in the $\Delta(1600)$ rest frame. In the S-state approach discussed in Sec. V, the amplitudes are given by Eqs. (24) and (25). The results are shown in Fig. 6. In the figure the contributions of the quark core (bare) are also shown. We predict from Fig. 6 that $A_{1/2}(Q^2)$ and
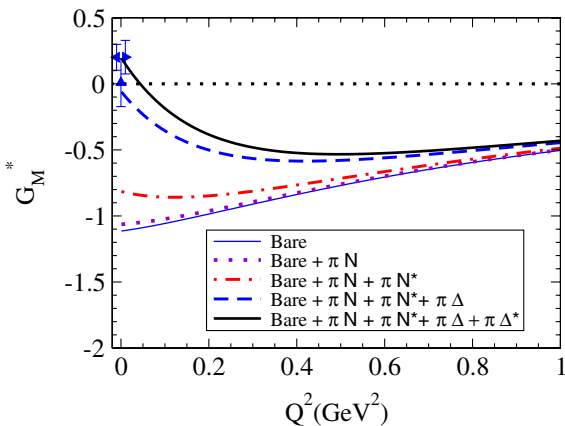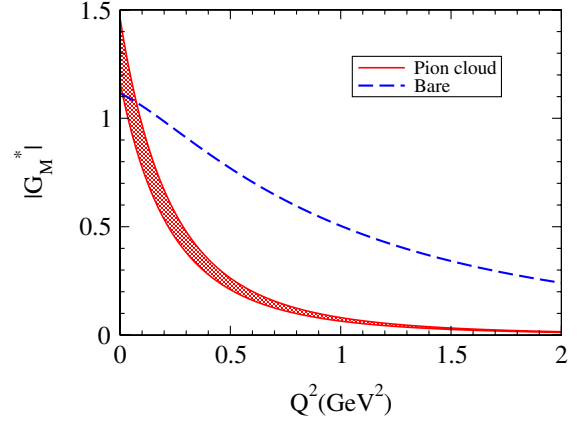

FIG. 4 (color online). Decomposition of the contributions for the $\gamma N \to \Delta(1600)$ magnetic dipole form factor.

$A_{3/2}(Q^2)$ become positive for $Q^2 > 0.1$ GeV^2. This result is consistent with the estimates made in Ref. [21], which are based on the valence quark structure. The positive sign in the helicity amplitudes for $Q^2 > 0.1$ GeV^2 is essentially a consequence of the quark core dominance.

D. Discussion

Our results for $G_M^*(0)$ (central value) are very close to the experimental data of Refs. [75,76]. The result is also consistent with the data of Awaji [20] within the error bars, but the data are not consistent with $G_E^* \equiv 0$ of the present approach. However, one should keep in mind that the present results are based on the approximation of ignoring the baryon mass differences in the estimate of the pion cloud contributions, and on the dominance of the photon-pion coupling diagram [diagram (a) in Fig. 1], which has a 10% ambiguity. Unfortunately, we cannot draw more definite conclusions, since the uncertainty associated with the pion cloud contributions is 0.148, which is comparable with the central value $G_M^*(0) = 0.202$, and also relatively large experimental errors exist. The large uncertainty in our estimate lies mainly in the $\pi\Delta$ intermediate state, in particular, the coupling constant $f_{\pi\Delta\Delta^*}$. An accurate value of the coupling constant would reduce the final uncertainty almost by a factor of 2. A better constraint of the pion cloud contribution can be achieved once better experimental data become available associated with the Δ^* decay to extract $f_{\pi\Delta\Delta^*}$. An alternative may be to use the coupling constants from an independent model for the meson-baryon interaction, where the coupling constants are constrained by many observables. At the moment such well-constrained coupling constants associated with the $\Delta(1600)$ are not available.

There is also uncertainty in the expression for the valence quark contributions G_M^b. In the Δ^* scalar wave function Eq. (13), there is an extra degree of freedom
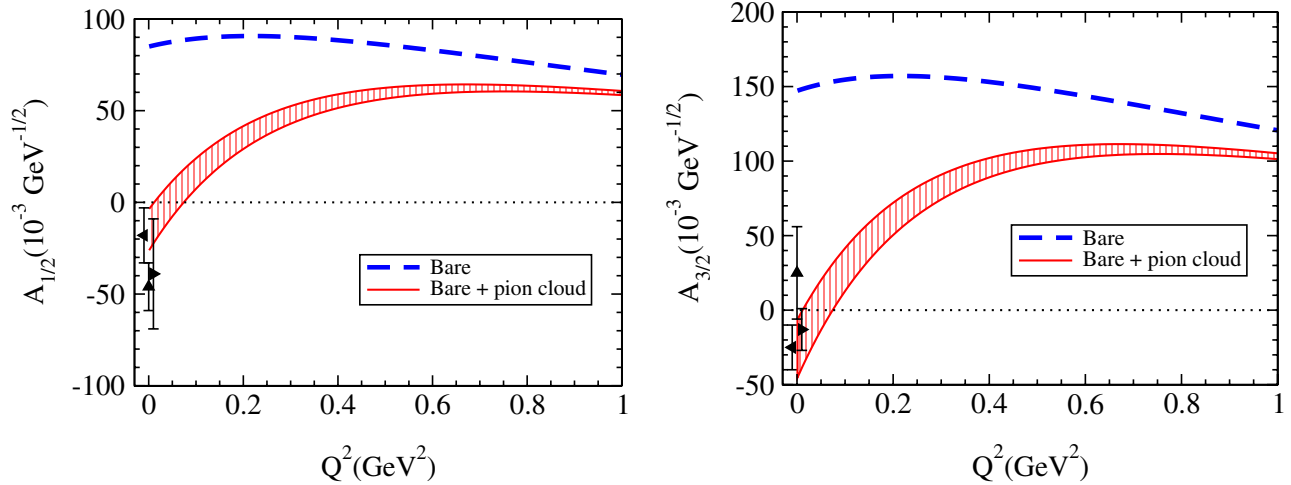
FIG. 6 (color online). Helicity amplitudes for the $\gamma N \rightarrow \Delta(1232)$ transition, calculated in the S-state approximation for the N and $\Delta(1600)$. Data from PDG [20]. See Table III.

associated with the momentum scale parameter α_3, which sets the scale of the variation of the Δ^* wave function compared to that of the ground state Δ. As explained in the text, we have fixed α_3 by the long-range scale parameter α_1 (same short-range structure for Δ and Δ^*). The choice, $\alpha_3 = \alpha_2$, would change the contributions of the core to $G_M^b(0) = -0.924$, to be compared with the result we have obtained, -1.113. An alternative method may be to adjust the parameters by fitting to the data of the helicity amplitudes or form factors, once they become available for finite Q^2. However, the advantage of the present approach to focus on the long-range scale parameter has also been proven to be good in the study of the $\gamma N \rightarrow P_{11}(1440)$ transition form factors [34].

VII. CONCLUSIONS

In this article, we have studied the $\Delta(1600)$ structure, and the $\gamma N \rightarrow \Delta(1600)$ transition using a covariant spectator formalism, with a simplified G_M^* dominance model. As far as the authors are aware, this is the first dynamical study for the $\gamma N \rightarrow \Delta(1600)$ transition including both the bare and meson cloud contributions. The role of the $\Delta(1600)$ resonance in the meson-baryon coupled-channel models has not been settled yet. Thus, theoretical study of this resonance can be a challenge for many baryon models. Our results show that solely the contributions from the quark core to the dominant form factor G_M^* at $Q^2 = 0$ are negative and far below the existing experimental data points, which are positive. However, the explicit inclusion of the pion cloud contributions overcome the negative contributions of the valence quark core to lead to the positive sign, which is consistent with the experimental positive values. The final result, although it has uncertainties associated with the coupling constants and approximations used, is consistent with the experimental data. Furthermore, the present study may provide a parametri-

zation for the Δ^* core that can be used in coupled-channel models.

It will be also very interesting to compare our estimate of the quark core contributions with the lattice QCD simulation data. Such simulations were performed in the past for the $\gamma N \rightarrow \Delta(1232)$ transition [55]. Finally, we have predicted the Q^2 dependence of the $G_M^*(Q^2)$ form factor. Based on the recent analysis for the electromagnetic structure of the $P_{11}(1440)$, $D_{13}(1520)$, $S_{11}(1535)$ and $S_{11}(1650)$, it is expected that also $P_{33}(1600)$ will be included in the multipole analysis in the near future.

The method used to estimate the pion cloud contributions is based on the processes that a photon couples directly to the pion, which may be justified by the previous study for the octet baryon magnetic moments in the same covariant spectator quark model, within about a 10% error. Then, based on the cloudy bag model formalism, we have made a connection for the pion cloud contributions between the $\gamma N \rightarrow \Delta(1232)$ and $\gamma N \rightarrow \Delta(1600)$ transitions, by summing over all the intermediate spin and isospin states. In this exploratory study, we have approximated the masses of all the intermediate state baryons by an average value of the N, $N(1440)$, Δ and $\Delta(1600)$. In the future we need to include explicitly the mass differences and treat the pion-baryon intermediate states properly.

We can apply the present valence quark model of the baryon with meson cloud dressing to other systems. One possibility is the $P_{11}(1440)$ and $P_{11}(1710)$ resonances, where the meson cloud dressing is expected to be very important in the small Q^2 region, since $P_{11}(1440)$ is described as the first radial excitation of the nucleon [34], and the $P_{11}(1710)$ resonance may also be considered as the second radial excitation of the nucleon [21]. Another possible application of the model may be to study the octet to decuplet baryon electromagnetic transitions, by extending the treatment for the $\gamma N \rightarrow \Delta(1232)$ to the SU(3) sector,

where the meson cloud dressing, pion, in particular, is also expected to be important [32,33].

APPENDIX: DECAY RATES AND COUPLING CONSTANTS ASSOCIATED WITH RESONANCES

In this appendix we calculate the coupling constants $f_{\pi BB'}$ necessary to estimate the pion cloud contributions based on the available experimental data [20]. The necessary coupling constants are $f_{\pi N\Delta}$, $f_{\pi NN(1440)}$, $f_{\pi N\Delta(1600)}$, $f_{\pi\Delta\Delta(1600)}$, and $f_{\pi N(1440)\Delta(1600)}$. For the other coupling constants, we use $f_{\pi NN} = 1$ ($f_{\pi NN}^2/4\pi = 0.08$) and the relation based on CBM [63,64], $f_{\pi NN} = f_{\pi\Delta\Delta} = f_{\pi\Delta(1600)\Delta(1600)}$. First, we present the effective Lagrangian densities used for the calculation of the coupling constants.

The Lagrangian densities used in the present study are

$$
\begin{aligned}
\mathcal{L}_{\pi NN} &= -\frac{f_{\pi NN}}{m_\pi}[\bar{N}\gamma^\mu\gamma_5\boldsymbol{\tau}N]\cdot\partial_\mu\boldsymbol{\pi}, \\
\mathcal{L}_{\pi NN^*} &= -\frac{f_{\pi NN^*}}{m_\pi}[\bar{N}^*\gamma^\mu\gamma_5\boldsymbol{\tau}N]\cdot\partial_\mu\boldsymbol{\pi} + \text{H.c.}, \\
\mathcal{L}_{\pi N\Delta} &= \frac{f_{\pi N\Delta}}{m_\pi}[\bar{N}\mathbf{T}\Delta^\mu]\cdot\partial_\mu\boldsymbol{\pi} + \text{H.c.}, \\
\mathcal{L}_{\pi N\Delta^*} &= \frac{f_{\pi N\Delta^*}}{m_\pi}[\bar{N}\mathbf{T}\Delta^{*\mu}]\cdot\partial_\mu\boldsymbol{\pi} + \text{H.c.}, \\
\mathcal{L}_{\pi N^*\Delta^*} &= \frac{f_{\pi N^*\Delta^*}}{m_\pi}[\bar{N}^*\mathbf{T}\Delta^{*\mu}]\cdot\partial_\mu\boldsymbol{\pi} + \text{H.c.}, \\
\mathcal{L}_{\pi\Delta\Delta^*} &= -\frac{f_{\pi\Delta\Delta^*}}{m_\pi}[\bar{\Delta}^\mu\gamma^\nu\gamma_5\mathbf{I}\Delta_\mu^*]\cdot\partial_\nu\boldsymbol{\pi} + \text{H.c.},
\end{aligned}
\tag{A1}
$$

where $\boldsymbol{\tau}$ are the Pauli matrices, and $\mathbf{T}$ and $\mathbf{I}$ are the isospin operators defined by $(\mathbf{T})_{Mm} \equiv \sum_\mu(1\mu\frac{1}{2}m|\frac{3}{2}M)\hat{e}_\mu^*$ and $(\mathbf{I})_{MM'} \equiv \frac{\sqrt{15}}{2}\sum_\mu(1\mu\frac{3}{2}M'|\frac{3}{2}M)\hat{e}_\mu^*$, respectively. Then, one can calculate decay rates and obtain the necessary coupling constants associated with the resonances. Widths, branching ratios, and calculated coupling constants of the resonances are summarized in Table I.

Next, we give expressions for decay rates calculated using the Lagrangian densities Eqs. (A1) to estimate the coupling constants.

The coupling constants are estimated from the decay rate expressions (see also Ref. [77]):

$$\Gamma(N(1440) \to \pi N)$$
$$= 3\frac{f_{\pi NN(1440)}^2}{4\pi}\frac{(M_N + M_{N(1440)})^2}{m_\pi^2}\frac{(E_N - M_N)|\vec{p}|}{M_{N(1440)}}, \tag{A2}$$

with

$$|\vec{p}| = \frac{\lambda^{1/2}(M_{N(1440)}^2, M_N^2, m_\pi^2)}{2M_{N(1440)}},$$

$$\Gamma(\Delta \to \pi N) = \frac{f_{\pi N\Delta}^2}{12\pi m_\pi^2}\frac{(E_N + M_N)|\vec{p}|^3}{M_\Delta}, \tag{A3}$$

with

$$|\vec{p}| = \frac{\lambda^{1/2}(M_\Delta^2, M_N^2, m_\pi^2)}{2M_\Delta},$$

$$\Gamma(\Delta(1600) \to \pi N) = \frac{f_{\pi N\Delta(1600)}^2}{12\pi m_\pi^2}\frac{(E_N + M_N)|\vec{p}|^3}{M_{\Delta(1600)}}, \tag{A4}$$

with

$$|\vec{p}| = \frac{\lambda^{1/2}(M_{\Delta(1600)}^2, M_N^2, m_\pi^2)}{2M_{\Delta(1600)}},$$

$$\Gamma(\Delta(1600) \to \pi N(1440))$$
$$= \frac{f_{\pi N(1440)\Delta(1600)}^2}{12\pi m_\pi^2}\frac{(E_{N(1440)} + M_{N(1440)})|\vec{p}|^3}{M_{\Delta(1600)}}, \tag{A5}$$

with

$$|\vec{p}| = \frac{\lambda^{1/2}(M_{\Delta(1600)}^2, M_{N(1440)}^2, m_\pi^2)}{2M_{\Delta(1600)}},$$

$$\Gamma(\Delta(1600) \to \pi\Delta)$$
$$= \frac{15}{4}\frac{f_{\pi\Delta\Delta(1600)}^2}{36\pi}\frac{(M_\Delta + M_{\Delta(1600)})^2}{m_\pi^2}\frac{M_\Delta|\vec{p}|}{M_{\Delta(1600)}}\left[\left(\frac{E_\Delta}{M_\Delta}\right) - 1\right]$$
$$\times\left[2\left(\frac{E_\Delta}{M_\Delta}\right)^2 - 2\left(\frac{E_\Delta}{M_\Delta}\right) + 5\right], \tag{A6}$$

with

$$|\vec{p}| = \frac{\lambda^{1/2}(M_{\Delta(1600)}^2, M_\Delta^2, m_\pi^2)}{2M_{\Delta(1600)}},$$

where, $\lambda(x, y, z) \equiv x^2 + y^2 + z^2 - 2xy - 2yz - 2zx$.

[1] V. D. Burkert and T. S. H. Lee, Int. J. Mod. Phys. E **13,** 1035 (2004).
[2] D. Drechsel, S. S. Kamalov, and L. Tiator, Eur. Phys. J. A **34,** 69 (2007).
[3] R. Arndt, W. Briscoe, I. Strakovsky, and R. Workman, Eur. Phys. J. A **35,** 311 (2008).
[4] I. G. Aznauryan, Phys. Rev. C **76,** 025212 (2007).
[5] I. G. Aznauryan et al. (CLAS Collaboration), Phys. Rev. C **80,** 055203 (2009).
[6] V. I. Mokeev, V. D. Burkert, T. S. H. Lee, L. Elouadrhiri, G. V. Fedotov, and B. S. Ishkhanov, Phys. Rev. C **80,** 045212 (2009).
[7] A. V. Anisovich, E. Klempt, V. A. Nikonov, M. A. Matveev, A. V. Sarantsev, and U. Thoma, Eur. Phys. J. A **44,** 203 (2010).
[8] M. Doring, E. Oset, and D. Strottman, Phys. Rev. C **73,** 045209 (2006).
[9] G. Penner and U. Mosel, Phys. Rev. C **66,** 055211 (2002); **66,** 055212 (2002).
[10] T. P. Vrana, S. A. Dytman, and T. S. H. Lee, Phys. Rep. **328,** 181 (2000).
[11] D. M. Manley, Int. J. Mod. Phys. A **18,** 441 (2003).
[12] S. S. Kamalov, S. N. Yang, D. Drechsel, O. Hanstein, and L. Tiator, Phys. Rev. C **64,** 032201(R) (2001).
[13] M. Doring, C. Hanhart, F. Huang, S. Krewald, and U. G. Meissner, Nucl. Phys. **A829,** 170 (2009).
[14] S. Schneider, S. Krewald, and U. G. Meissner, Eur. Phys. J. A **28,** 107 (2006).
[15] T. Sato and T. S. H. Lee, Phys. Rev. C **63,** 055201 (2001).
[16] B. Julia-Diaz, T. S. H. Lee, A. Matsuyama, and T. Sato, Phys. Rev. C **76,** 065201 (2007).
[17] A. Matsuyama, T. Sato, and T. S. Lee, Phys. Rep. **439,** 193 (2007).
[18] B. Julia-Diaz, T. S. H. Lee, T. Sato, and L. C. Smith, Phys. Rev. C **75,** 015205 (2007).
[19] S. Capstick, Phys. Rev. D **46,** 2864 (1992).
[20] C. Amsler et al. (Particle Data Group), Phys. Lett. B **667,** 1 (2008).
[21] S. Capstick and B. D. Keister, Phys. Rev. D **51,** 3598 (1995).
[22] B. Golli and S. Sirca, Eur. Phys. J. A **38,** 271 (2008).
[23] T. Skorodko et al., Phys. Lett. B **679,** 30 (2009).
[24] T. Skorodko et al. (for the CELSIUS/WASA Collaboration and for the CELSIUS/WASA Collaboration), AIP Conf. Proc. **1257,** 520 (2010).
[25] X. Cao, B. S. Zou, and H. S. Xu, Phys. Rev. C **81** 065201 (2010).
[26] G. Engel, C. Gattringer, C. B. Lang, M. Limmer, D. Mohler, and A. Schafer, arXiv:0910.2802.
[27] D. B. Leinweber, W. Melnitchouk, D. G. Richards, A. G. Williams, and J. M. Zanotti, Lect. Notes Phys. **663,** 71 (2005).
[28] G. Erkol and M. Oka, Nucl. Phys. **A801,** 142 (2008).
[29] F. Gross, G. Ramalho, and M. T. Peña, Phys. Rev. C **77,** 015202 (2008).
[30] F. Gross, G. Ramalho, and M. T. Peña, Phys. Rev. C **77,** 035203 (2008).
[31] G. Ramalho, M. T. Peña, and F. Gross, Eur. Phys. J. A **36,** 329 (2008).
[32] G. Ramalho, M. T. Peña, and F. Gross, Phys. Rev. D **78,** 114017 (2008).
[33] G. Ramalho and M. T. Peña, Phys. Rev. D **80,** 013008 (2009).
[34] G. Ramalho and K. Tsushima, Phys. Rev. D **81,** 074020 (2010).
[35] G. Ramalho and M. T. Pena, J. Phys. G **36,** 115011 (2009).
[36] G. Ramalho and M. T. Peña, J. Phys. G **36,** 085004 (2009).
[37] G. Ramalho, M. T. Peña, and F. Gross, Phys. Lett. B **678,** 355 (2009); Phys. Rev. D **81,** 113011 (2010).
[38] G. Ramalho, K. Tsushima, and F. Gross, Phys. Rev. D **80,** 033004 (2009).
[39] F. Gross, G. Ramalho, and K. Tsushima, Phys. Lett. B **690,** 183 (2010).
[40] H. F. Jones and M. D. Scadron, Ann. Phys. (N.Y.) **81,** 1 (1973).
[41] C. Becchi and G. Morpurgo, Phys. Lett. **17,** 352 (1965).
[42] N. Isgur, G. Karl, and R. Koniuk, Phys. Rev. D **25,** 2394 (1982).
[43] V. Pascalutsa, M. Vanderhaeghen, and S. N. Yang, Phys. Rep. **437,** 125 (2007).
[44] A. N. Villano et al., Phys. Rev. C **80,** 035203 (2009).
[45] A. Faessler, T. Gutsche, B. R. Holstein, V. E. Lyubovitskij, D. Nicmorus, and K. Pumsa-ard, Phys. Rev. D **74,** 074010 (2006).
[46] J. Rohrwild, Phys. Rev. D **75,** 074025 (2007).
[47] V. M. Braun, A. Lenz, G. Peters, and A. V. Radyushkin, Phys. Rev. D **73,** 034020 (2006).
[48] L. Wang and F. X. Lee, Phys. Rev. D **80,** 034003 (2009).
[49] T. A. Gail and T. R. Hemmert, Eur. Phys. J. A **28,** 91 (2006).
[50] V. Pascalutsa and M. Vanderhaeghen, Phys. Rev. D **73,** 034003 (2006).
[51] Y. B. Dong, K. Shimizu, A. Faessler, and A. J. Buchmann, Phys. Rev. C **60,** 035203 (1999).
[52] P. Alberto, L. Amoreira, M. Fiolhais, B. Golli, and S. Sirca, Eur. Phys. J. A **26,** 99 (2005).
[53] D. Y. Chen and Y. B. Dong, Commun. Theor. Phys. **50,** 142 (2008).
[54] U. G. Meissner, AIP Conf. Proc. **904,** 142 (2007).
[55] C. Alexandrou, G. Koutsou, H. Neff, J. W. Negele, W. Schroers, and A. Tsapalis, Phys. Rev. D **77,** 085012 (2008).
[56] C. Savkli and F. Gross, Phys. Rev. C **63,** 035208 (2001).
[57] F. Gross and P. Agbakpe, Phys. Rev. C **73,** 015203 (2006).
[58] B. Julia-Diaz, D. O. Riska, and F. Coester, Phys. Rev. C **69,** 035212 (2004); **75,** 069902(E) (2007).
[59] I. G. Aznauryan, V. D. Burkert, and T. S. Lee, arXiv:0810.0997.
[60] M. M. Giannini, Rep. Prog. Phys. **54,** 453 (1991).
[61] D. Arndt and B. C. Tiburzi, Phys. Rev. D **69,** 014501 (2004).
[62] I. C. Cloet, D. B. Leinweber, and A. W. Thomas, Phys. Lett. B **563,** 157 (2003).
[63] A. W. Thomas, S. Theberge, and G. A. Miller, Phys. Rev. D **24,** 216 (1981).
[64] A. W. Thomas, Adv. Nucl. Phys. **13,** 1 (1984).
[65] L. R. Dodd, A. W. Thomas, and R. F. Alvarez-Estrada, Phys. Rev. D **24,** 1961 (1981).
[66] S. Theberge and A. W. Thomas, Nucl. Phys. A **393,** 252 (1983).
[67] A. W. Thomas, Prog. Theor. Phys. **168,** 614 (2007).

[68] K. Tsushima, T. Yamaguchi, Y. Kohyama, and K. Kubodera, Nucl. Phys. **A489**, 557 (1988).

[69] T. Yamaguchi, K. Tsushima, Y. Kohyama, and K. Kubodera, Nucl. Phys. **A500**, 429 (1989).

[70] K. Kubodera, Y. Kohyama, K. Oikawa, and C. W. Kim, Nucl. Phys. **A439**, 695 (1985).

[71] D. H. Lu, A. W. Thomas, and A. G. Williams, Phys. Rev. C **55**, 3108 (1997).

[72] D. H. Lu, A. W. Thomas, and A. G. Williams, Phys. Rev. C **57**, 2628 (1998).

[73] D. H. Lu, S. N. Yang, and A. W. Thomas, Nucl. Phys. **A684**, 296 (2001).

[74] D. O. Riska and G. E. Brown, Nucl. Phys. **A679**, 577 (2001).

[75] R. l. Crawford and W. t. Morton, Nucl. Phys. **B211**, 1 (1983).

[76] R. A. Arndt, I. I. Strakovsky, and R. L. Workman, Phys. Rev. C **53**, 430 (1996).

[77] K. Tsushima, A. Sibirtsev, A. W. Thomas, and G. Q. Li, Phys. Rev. C **59**, 369 (1999); **61**, 029903(E) (2000).